DESIGN AND ANALYSIS OF SELF-DRIVING ARTICULATED SOFT ACTUATOR

Shuqi Wang,* Jizhuang Fan,* Yitao Pan,* and Yubin Liu*

Abstract

The pneumatic soft actuator has a great influence on the structural design of robot. However, the robot has the disadvantages of complex structure, heavy weight and a shorter sustainable locomotion time due to the soft actuator needs to be equipped with an external air cylinder. Here, we present a self-driving articulated soft actuator (SASA) to solve this problem. The proposed actuator consists of a linear and a semicircular soft chamber, which is bonded by non-stretchable material. The stretch and recovery motion of the SASA can be realised by controlling a solenoid valve and a one-way pump to adjust the flow direction of the pre-charged air. A deformation analysis model is performed to characterise several structural parameters and their effect on drive performance. Details on design decisions and experimental results analysis are presented based on trajectory planning. While reducing the overall mass and ensuring the motion efficiency, the actuator greatly improves the sustainable locomotion time. Meanwhile, the structure and control principle of the SASA can also provide a reference for the design of other soft robots without external sources.

Key Words

Articulated soft actuator, self-driving, bionic limbs, sustainable locomotion

1. Introduction

Biological frogs can achieve intermittent and high-explosive swimming by means of coordinated stroke and propulsion of limbs [1], [2]. Compared with other underwater propulsion mechanisms, this swimming method has strong manoeuverability and better movement stability [3], [4]. Most of the traditional frog-inspired swimming limbs are mainly made of rigid materials, which not only have a heavy weight but also reduce the environmental adaptability of the robot [5]–[7]. One of the development trends of limbs is to integrate the advantages of light weight and high flexibility of soft materials for bionic structure design [8]–[11]. Due to the novel actuators based on dielectric elastomer and shape memory alloy have certain shortcomings in manufacturing process and motion efficiency, it is not suitable for the development of swimming limbs [12], [13]. The traditional driving methods, such as servo motors and pneumatic muscles are gradually replaced by novel soft actuators [14]–[17].

Soft actuators are a buzzword in recent robotic researches [18]–[21]. It is a device that executes a transformation process from a power to a mechanical power through the deformation of materials in a particular structure. The power generator and actuator are integrated into the power-actuator system in most cases [22]. A frog-inspired swimming limb based on soft actuators has been successfully developed [23]. The actuators commonly used in soft robotics are soft pneumatic actuators (SPAs), which are actuated by the use of compressed air. In particular, bending SPAs derive their deflection with progressively smaller curvature due to the air pressure built within their chambers. This bending motion is suitable for a diverse set of applications, such as gripping and manipulating irregular objects [24], adaptable locomotion in unstructured environments [25]. The bending SPAs have the advantages of simple operation mode, high driving efficiency and strong adaptability, which can just make up for the existing deficiencies of the bionic limbs [26]. The limb's kinematic analysis and prototype swimming experiments have been performed to verify the feasibility and rationality of a swimming robot based on bending SPAs as the limbs driving units [27]. However, once inflated with pressurised air begins to move, SPAs suffer from its inherent disadvantage of requiring an external air source and a pressure-stabilising valve, which results in a complex structure and heavy weight of the robot. The most important thing is that this reduces the sustainable motion time, which greatly affects the motion performance of the robot. In addition, although fibre wires can be manually wound on the outer surface of the elastic matrix to limit the radial deformation of the bending SPAs to improve its driving capability [28], the complex preparation process makes it difficult to manufacture the actuators in batches [29]. To circumvent these issues faced by SPAs

* State Key Laboratory of Robotics and System, Harbin Institute of Technology, Harbin, Heilongjiang 150001, China; e-mail: wangshuqi@hit.edu.cn; fanjizhuang@hit.edu.cn; 21b308005@stu.hit.edu.cn; liuyubin@hit.edu.cn
Corresponding authors: Shuqi Wang, Yubin Liu

(DOI: 10.2316/J.2024.206-1038)

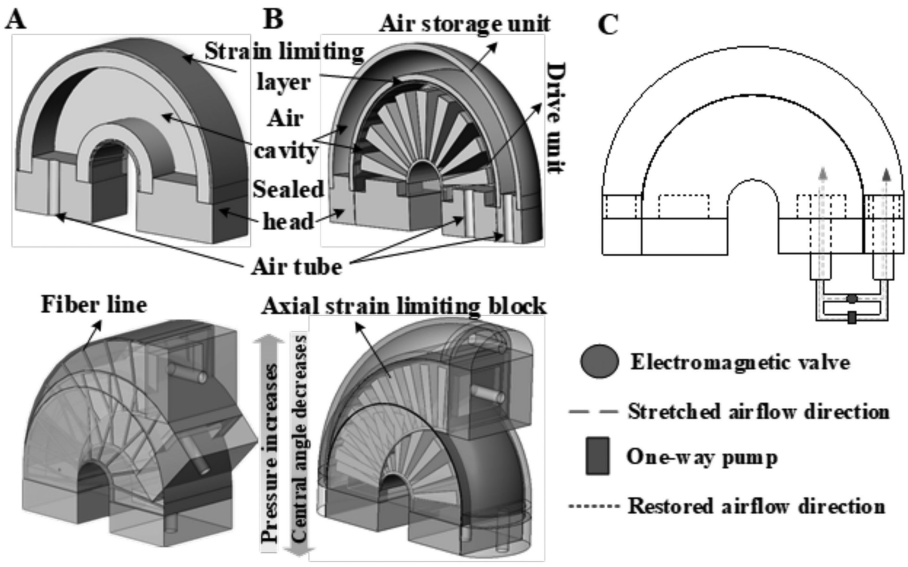

Figure 1. (a) Comparison between a traditional soft pneumatic actuator; (b) the proposed soft actuator. Both the central angle and the curvature vary with the air pressure. (c) The schematic diagram of the actuation principle of the SASA.

upon inflation, some solutions have been proposed to the shortage of compressed air [30], [31]. Deriving inspiration from the weighing scale, where the air chamber of the actuator is pre-charged with compressed air and combined with tendon-driven to guide its motion along a predefined desired trajectory [32].

This work presents a new type of self-driving articulated soft actuator (SASA) in an effort to circumvent some of the above-mentioned drawbacks faced by conventional SPAs for bionic limbs. We have improved the air supply method by changing the structure of the soft actuator, so that the SASA does not need to be equipped with an external independent air source during movement, and improves the sustainable locomotion time by relying on its own air circulation. In addition, the novel actuator does not need to wound with fibre wires, which simplifies the preparation process and shortens the preparation time. On this basis, the structural model of the soft actuator is established, and its structural parameters are optimised and analysed. The SASA presented here comprises a bending SPA core, to mimic the curled state of the joints before locomotion, and a linear air storage unit that provide the necessary compressed air for actuation motion. The SASA integrates rigid and soft material, and the tensile strength and hardness of each part and interface are also different, which enhances its adaptability to the environment. The rationality of the soft actuator is verified, and its structure and locomotion principle can provide a reference for the design of other soft robots without external sources.

In the following sections, analysis related to the design and the locomotion principles for the SASA is described. Subsequently, analysis and testing for the integrated bionic limbs comprising multiple actuators are shown in context of the performance achieved. Finally, a discussion of the results is provided.

2. Design and Preparation

2.1 Structure Design

Aiming at the existing problems of soft actuators, a self-pumping articulated pneumatic soft actuator is designed to realise the miniaturisation, lightweight, and sustainable motion of bionic limbs. Combined with the characteristics of the contracted joints before locomotion, the initial shape of the traditional articulated pneumatic soft actuator is designed as a semi-annular as shown in Fig. 1a. Bending motion can be achieved by the strain difference between the non-stretchable material and the elastic matrix when the compressed air is charged into the soft actuator. A novel SASA is proposed based on the traditional articulated pneumatic soft actuator, which mainly includes air storage unit, driving unit, sealing blocking head, air guiding blocking head, and a non-stretchable material, as shown in Fig. 1b. The linear air storage unit with a semicircular cross-section and the semi-annular driving unit with a rectangular cross-section are arranged up and down, and the outer surfaces are, respectively, adhered to the hard plate-like strain limiting layer sheets with bending elasticity. In this way, the shape of the SASA becomes more compact and the overall volume is smaller while ensuring sufficient amount of air. With the help of the uniform arrangement of strain limiting blocks inside the drive unit to limit the radial deformation, processes, such as the manual winding of fibre wires and secondary pouring are avoided, which simplifies the process flow and makes batch production possible. Although the proposed approach adopts the commonly practiced structures for the SASA design, an external air cylinder is no longer required once the air storage unit is pre-charged with compressed air. With the help of two tee connectors and tubes, a one-way pump and a solenoid valve are connected in parallel

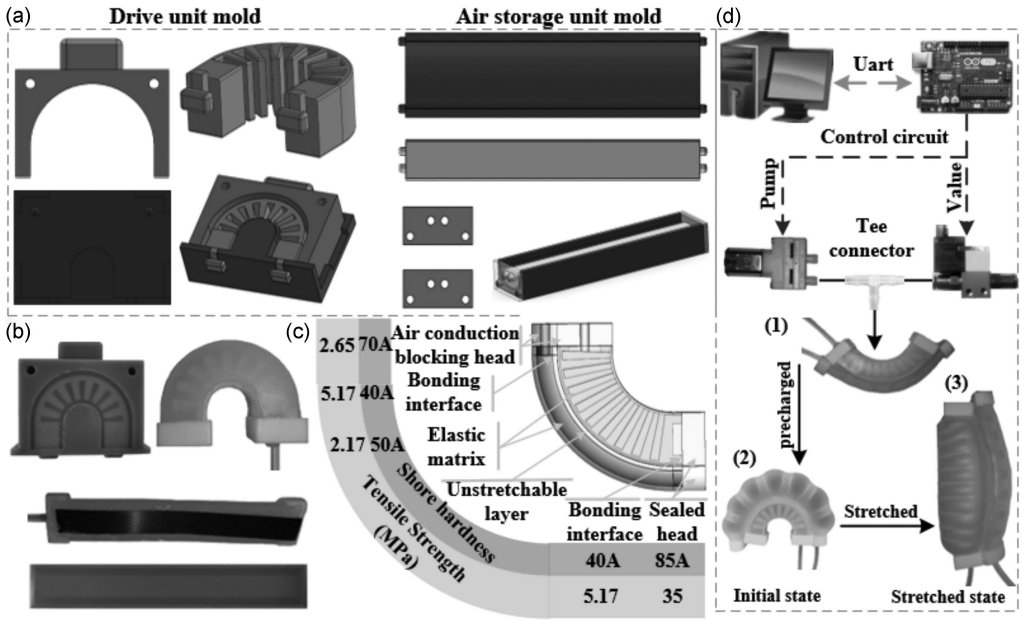

Figure 2. Design and the control system of the SASA: (a) 3D model of the soft actuator mould; (b) top view of the two units of the actuator; (c) the tensile strength and hardness distribution of the soft actuator; and (d) control system: (1) state after bonding; (2) initial state after pre-inflation; and (3) the stretched state.

between the two chambers through the air guiding blocking heads, as shown in Fig. 1c. It should be noted that the ventilation direction of the one-way pump is from the drive unit to the air storage unit. The articulated pneumatic soft actuator can drive the bionic limb to achieve a more intense limb extension movement in the propulsion stage and a gentler movement in the recovery stage by using the moment generated by the pressure difference and the recovery strain of the elastic matrix. As an important unit of the structure design, the proposed SASA is also the driving unit of leg movement while acting as a limb joint and connecting component, which helps to realise the compactness of the bionic limb.

2.2 Preparation Process

The entire preparation process of the soft actuator only includes mould design and three-dimensional (3D) printing, casting, bonding, *etc.* The 3D schematic diagram of the mould for each unit of the proposed prototype SASA and its assembly process is shown in Fig. 2a. The elastic base is cast with Eco-flex 0050 with a hardness of 50A, and the actuator blocking head is cast with Sylgard-184 to prevent invalid deformation of the end when the pressure in the air chamber is large. In addition, as a key component of the actuator, the 0.15 mm steel sheet is used as a strain limiting material to provide a restoring elastic force during the stretching motion to assist the actuator to stretch while limiting the strain. Meanwhile, the rigid material is embedded in the soft elastic matrix as shown in Fig. 2b, so that the actuator has both the flexibility of the soft material and the load-bearing capacity of the rigid material, which improves the motion efficiency and the adaptability to the external environment. Adhesive bonding is used to connect the elastic matrix, blocking heads and strain limiting layer to form an actuator that combines rigid and soft properties, as shown in Fig. 2c (Smooth-On Sil-Poxy Silicone Adhesive).

2.3 Actuation Principle

The actuation principle and control system are very easy and simple, as shown in Fig. 2d. The control philosophy is that the air pressure difference between the two units is controlled by the on–off of the solenoid valve and the pumping of the one-way pump to realise the bending angle change of the actuator and then realise the stretching and contraction motion of the bionic limbs. The air storage unit is pre-charged with air, and the one-way pump and solenoid valve are both closed as the initial state. Due to the combined action of the strain limiting layer and the pre-charged air, the linear air storage unit is deformed into a semi-circular shape, which also drives the non-stretchable material to produce bending deformation. Combined with the initial state of the drive unit, the SASA at this time is also in the shape of a semi-annular as a whole, which conforms to the frog's biological characteristics of being bent and contracted before swimming. Only the solenoid valve is opened first when starting the stretching movement, so that the high-pressure air in the air storage unit enters the driving unit, and the stretching movement with the center angle gradually decreasing is realised together with the restoring elastic force of the strain limiting layer and air storge unit. The torque generated by the soft actuators can drive the bionic limbs to realise the water-swiping motion. The solenoid valve is closed and the one-way pump is opened at the beginning of the recovery motion, and the air in the drive unit is pumped to the air storage unit to generate air pressure difference. In conjunction with the restoring force of the drive unit,

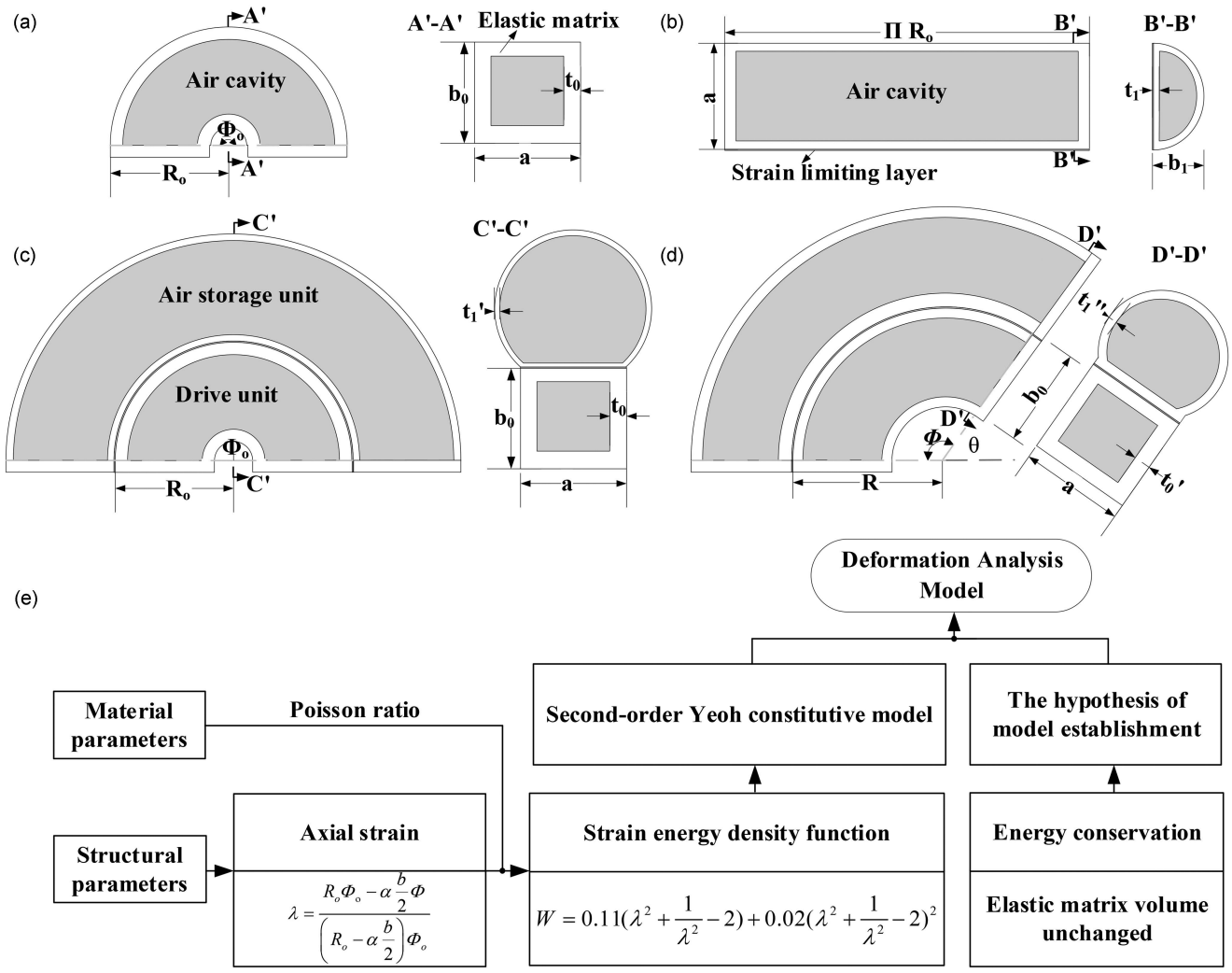

Figure 3. Deformation analysis model of the soft actuator; (a) structural parameters of the drive unit; (b) structural parameters of the air storage unit; (c) structural model of the actuator in the initial state; (d) structural model of the motion state; and (e) the block flowchart of the deformation analysis model.

the SASA can be driven to restore its initial state. At this point, close the one-way pump to complete a cycle. Such internal air can be recycled and reused without the need for an additional external air source, which improves the time of sustainable locomotion. This kind of soft actuator is driven by its own internal air, realising the air self-sufficiency, acting as a driving component and also serving as a joint of the limb. This is why the proposed actuator is called SASA. Similar to the concept integrated micro fluidic circuit (IMC), but the medium is different [33].

3. Analytical Modelling

A key point of the proposed SASA is the effect of structural parameters on the volume and pressure of the actuator chambers during motion. The following provides a theoretic modelling of such effect. The unit and overall structural model of the proposed SASA are shown in Fig. 3, and the structural parameters $\{R_o, \Phi_o, a, b_0, b_1, t_0, t_1\}$ of the two units are modelled and analysed. The initial shapes of the two units before bonding are linear and semi-circular, respectively. After the air storage unit is pre-filled with air, the structural model and parameters of the soft actuator in the initial state are shown in Fig. 3c, and its structural parameters change with the air pressure of the chamber during motion.

3.1 Deformation Analysis Model

The gas storage unit produces a bending motion under the action of the compressed gas and the strain limiting layer, while the driving unit produces an extension motion on the contrary. Although the movement trends of the two units are opposite, the movement principles are similar. Since the structural parameters of the drive unit have a direct impact on the performance of the soft actuator, the model deformation analysis is carried out by taking the drive unit as an example. Its deformation model can be referred to the lower part of Fig. 3c and d. To simplify the analysis, we assume that under the action of the strain limiting layer and the inner strain limiting block, the drive unit of the SASA has no radial expansion, that is, the outer contour size of the section remains unchanged. The overall volume of the elastic matrix remains unchanged during the

deformation process and the deformation curvature and the rubber material of the air chamber change uniformly.

Based on the above assumptions, a schematic diagram of the structural parameters of the drive unit is shown in Fig. 3. In the absence of external forces and when the drive unit is filled with compressed gas to reach a stable state, the work done by the compressed gas is completely used to overcome the internal stress of the rubber material, and the equilibrium expression can be established as follows:

$$P_{\text{in}} dV_c = V_r \text{dW} \tag{1}$$

Where, P_{in} is the pressure of the input gas; V_c is the air chamber volume of the drive unit when the bending angle is Φ; V_r is the overall volume of the elastic matrix, which is a constant after the structural parameters are determined.

The equivalent relationship between the volume of the actuator cavity, the elastic matrix, and the total volume during the deformation process is as follows:

$$V_r = V_d - V_c = f(t, \Phi) \tag{2}$$

Where, V_d is the total volume of the soft actuator at the bending angle; t is the rubber thickness of the outer wall of the air chamber during the deformation of the actuator.

Since the overall volume of the elastic matrix remains unchanged during the stretching process, the volume of the air chamber V_c when the bending angle is Φ can be determined according to the change of its geometric parameters, and then the volume change dV_c of the air chamber can be obtained.

$$V_c = \int_0^{\Phi} \int_{R-b+t}^{R-t} \text{ardrd}\theta \tag{3}$$

The Yeoh model is a reduced polynomial model based on Rivlin's phenomenological theory of rubber elasticity, which has a good predictive effect. Combined with the approximate incompressibility of the rubber material (Poisson's ratio μ is 0.47), the Yeoh constitutive model applied to the drive unit can be obtained as:

$$W = 0.11\left(\lambda^2 + \frac{1}{\lambda^2} - 2\right) + 0.02\left(\lambda^2 + \frac{1}{\lambda^2} - 2\right)^2 \tag{4}$$

Where, λ is the axial strain. According to the structural parameters of the actuator, it can be expressed as:

$$\lambda = \frac{R_o\Phi_o - \alpha\frac{b}{2}\Phi}{\left(R_o - \alpha\frac{b}{2}\right)\Phi_o} \tag{5}$$

Where, α is a correction parameter, which is used to reasonably determine the position of axial principal strain. Based on the above analysis, the relationship between the bending angle Φ of the drive unit and the input gas pressure P_{in} is obtained as follows:

$$P_{\text{in}} = \frac{\left(2R_o b - b^2 + (R_o - b)(a - 2t_o)\right)\Phi_o t_o \frac{\text{dW}}{d\Phi}}{\left(bt - \frac{t^2}{2} - (R_o\Phi_o - b\Phi + t\Phi)\frac{\text{dt}}{d\Phi}\right)} \tag{6}$$

Combined with the strain energy density function of the Yeoh constitutive model and the structural parameters of the soft actuator, a mathematical model is established by using the idea of the virtual work principle. The relationship between the input air pressure and the bending angle of the soft actuator is established from the perspective of energy conservation in the deformation process. It can be seen from (6) that the variables are all related to the bending angle Φ of the articulated pneumatic soft actuator. The block diagram of the modelling analysis process is shown in Fig. 3e. Combining the strain energy density function of the second-order Yeoh constitutive model and the structural parameters of the soft actuator, the mathematical model is established by using the principle of virtual work. From the perspective of energy conservation in the deformation process, the relationship between the input air pressure and the bending angle of the soft actuator is obtained.

3.2 Parameter Optimisation

To realise the compactness and light weight of the limb structure, the initial structure parameters $\{R_o,\ \Phi_o,\ a\}$ = {20 mm, π, 18 mm} of the SASA are determined as constant according to the size of the biological limbs. Combined with the deformation analysis model, it can be seen that the performance of the drive unit is mainly affected by the structural parameters $\{b_0, b_1, t_0, t_1\}$.

To further analyse the influence of structural parameters on the motion performance of the SASA, the initial thickness t_0 = 1.5 mm and section width d_0 = 13 mm of the upper air storage unit are, respectively, controlled, and the initial thickness and section width of the drive unit are t_1 = 1.5 and d_1 = 11, respectively. The effect of these design factors is investigated, and the P_{in}-Φ characteristic curves of the chamber of the two units with different initial thicknesses and the cross-sectional width are studied, as shown in Fig. 4a and b. It can be seen that when other parameters remain unchanged, with the decrease of the section width or the increase of thickness of the air chamber, the greater the input air pressure required to achieve the same bending angle. The influence of these structural parameters can be intuitively recognised from the characteristic curve, but it cannot be used to accurately determine its final structural parameters.

3.3 Moment Analysis

The SASA not only acts as a connecting piece but also used as a driving element for the legs. With the cooperation of several actuators, it drives the bionic limbs to overcome water resistance to achieve paddling locomotion and restore the initial state. The high-pressure air in the upper air storage unit is the key to the extension movement of the SASA. The air storage unit allows for the extension of the drive unit while simultaneously providing a restoring force that accelerates the actuator extension to a desirable angle. As shown in Fig. 4c, the air storage unit can maintain the bending angle Φ when there is no external force, and the moment M_P generated by the internal air pressure at the end is balanced with the moment M_r generated by the stress in the elastic matrix. When it is

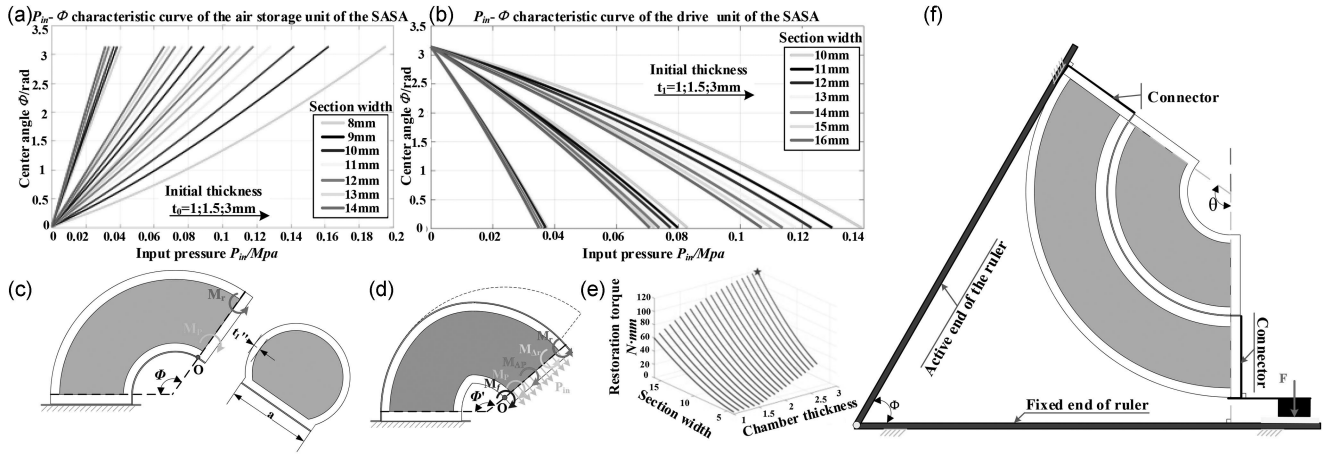

Figure 4. The characterisation of the actuator: (a) characteristic curve of the air storage unit; (b) characteristic curve of the drive unit. The curves of different colours represent different section widths, and are divided into three groups from left to right, each representing a different initial thickness. Their central angle changes oppositely. (c) The torque equilibrium state without external force; (d) the torque equilibrium state with external force; (e) the effect of structural parameters on the restoration torque; and (f) schematic diagram of torque measurement.

acted by the external resistance torque M_f and reaches the equilibrium state again, as shown in Fig. 4d, the bending angle Φ decreases and the internal air pressure increases, so that the elastic matrix material generates a torque increase $M_{\Delta r}$ due to the extrusion deformation, and the torque generated by the internal air pressure increases $M_{\Delta P}$. At this time, the torque M_D relative to point O can be regarded as the propulsion torque generated by the air storage unit, and the torque can be expressed as:

$$M_D = M_P + M_{\Delta \mathrm{P}} + M_r + M_{\Delta r} = M_{\Delta \mathrm{P}} + M_{\Delta r} = M_f \quad (7)$$

Since the air storage unit is in the process of releasing pressure during the extension process, it is not possible to increase the driving torque by increasing the internal air pressure in the chamber. In addition, M_r is only related to its structural parameters when the elastic matrix material and bending angle of the air storage unit are constant. Therefore, to make it provide the maximum driving torque at the same bending angle, the structural parameters of the air storage unit are determined with the goal of the maximum restoring torque on the premise of ensuring the minimum air pressure value required for the extension movement of the drive unit. The torque analysis principle of the drive unit of the SASA is the same. To enable the drive unit to provide as large a restoring torque as possible at the same bending angle to reduce the power demand for the one-way pump during the restoration movement, the structural parameters of the drive unit are also determined with the goal of the maximum restoring torque, as shown in Fig. 4e. According to the above analysis results, the overall structural parameters of the SASA are finally determined as $\{Ro, \Phi o, a, b0, t0, b1, t1\} = \{20$ mm, π, 18 mm, 16 mm, 3 mm, 9 mm, 3 mm$\}$.

The size of the torque has a great influence on the propulsion movement of the bionic limb. To better understand the driving torque characteristics of the SASA, the mechanical properties of the soft actuator under external load are obtained by experimental test. The schematic diagram is shown in the Fig. 4f. The active end adopts a digital display angle ruler with a resolution of 0.05°, which is used to indirectly measure the central angle of the soft actuator. The pressure sensor is used to measure the positive pressure on the end connector of the SASA. The driving torque of the actuator is about 45 N·mm by averaging multiple measurements. Subsequent experiments will be carried out to further verify the rationality of the bionic limb structure design and locomotion principle.

4. Results and Discussion

4.1 Trajectory Planning

By analysing the movement law of the joints in each stage of frog swimming, the posture sequence of the bionic limb model can be obtained, as shown in Fig. 5a, in which the right limb posture sequence shows the propulsion motion sequence, and the left limb posture sequence shows the recovery motion sequence. The black curve is expressed as the soft actuator under different bending states. In the propulsive stage, the flipper is perpendicular to the direction of motion to increase the thrust based on resistance. In the recovery stage, the flipper is parallel to the direction of motion for a long time to achieve the goal of reducing the greater recovery resistance of the limb. From the perspective of practical application, this will help to improve the efficiency of bionic limb movement.

Once the SASA with two units is assembled, several experiments are carried out to test its motion performance. These tests are aimed at verify the feasibility of using SASA for bionic limbs based on trajectory planning. The control sequence for each SASA of the limb is shown in Fig. 5b. From the deformation analysis of the actuator, it can be seen that the bending angle of the actuator is related to the air pressure in each unit, and the trajectory of the bionic limb is closely related to the bending angle of the actuator, so we can control the air pressure difference to control the

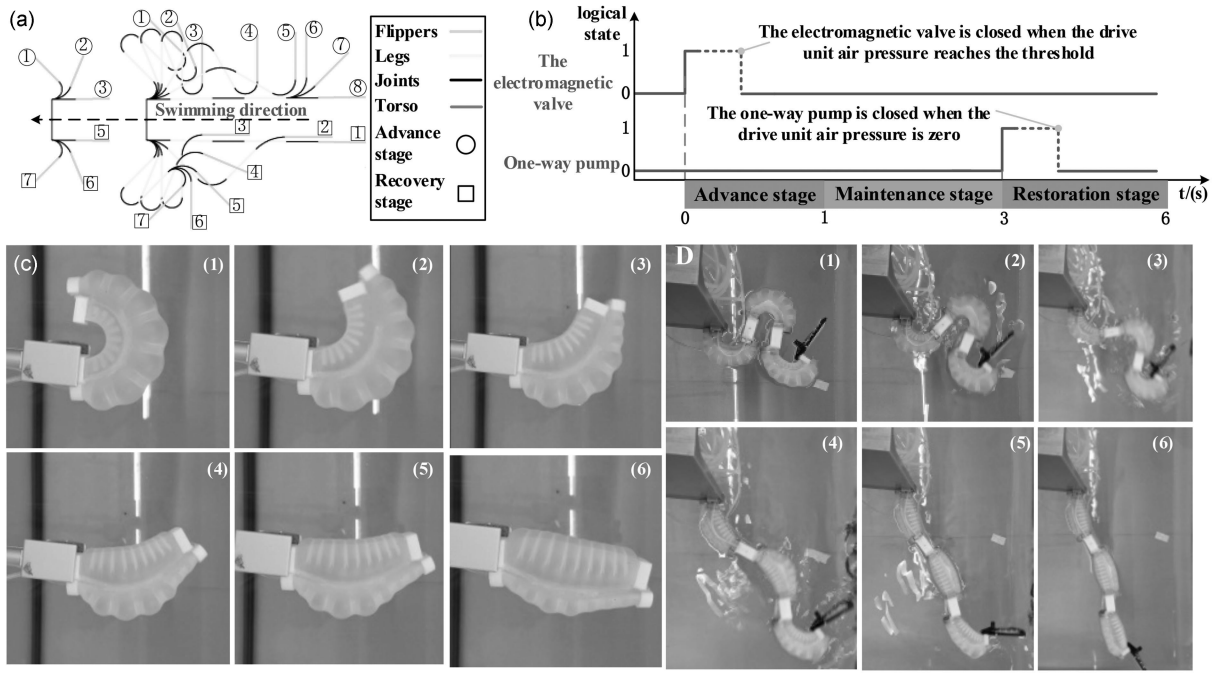

Figure 5. (a) Trajectory planning of limbs in two movement phases. The black curve is expressed as the soft actuator under different bending states; (b) the working procedure of control device. The working time and sequence can be adjusted at any time to adjust the pressure difference between the two units to adapt to different structural parameters; (c) single-joint experimental verification; and (d) multi-joint experimental verification.

trajectory of the bionic limb. Air pressure can be adjusted by only one solenoid valve and one-way pump. It is worth noting that the working time and working sequence of these two components can be adjusted at any time to adapt to different structural parameters and motion states.

4.2 Joint Verification

One end of the actuator is connected to the support to simulate the forelimb movements during the propulsion and recovery phases, as shown in the Fig. 5c. With the cooperation of the solenoid valve and the one-way pump, the actuator can achieve free flexion and extension movements. Since the most important feature of the actuator is that it can be repeatedly driven by pre-charged air without an external air source, the air tightness of the actuator is very important. The cyclic motion test of the actuator is carried out based on the forelimb motion experiment. After several cycles of motion, the air pressure in the air storage unit of the actuator can still be maintained stable, which not only meets the driving requirements but also realises the recycling of air.

The bionic hindlimb structure is shown in the Fig. 5d, which includes three SASAs as each joint, as well as structures such as thighs, legs, and flippers. Adjust the air pressure in the inner cavity of each actuator according to the control process, and realise the coordinated action of the actuators by controlling the one-way pump and solenoid valve of each soft actuator. It can be seen that the extension and recovery movements of the hind limbs are relatively flexible, and there is no stuttering phenomenon, which indicates that it can approximate the stroke of the frog's limbs, and further verifies the rationality of the actuator structure and the feasibility of the bionic limbs.

5. Conclusion

In this research, we have presented a SASA and design a frog-inspired swimming leg. The SASA is used for the connection and drive component of the limb, and its overall structure and fabrication process are very simple. In addition, the actuator combines the properties of rigid and soft materials that increase the adaptability of the limb to the environment. Major design innovations are in the following three aspects: (1) Two units with different cross-sections and initial shapes are arranged above and below to form the SASA and (2) adding internal strain limiting blocks instead of manual winding of fibre wires simplifies the fabrication process, and (3) replacement of the bulky pneumatic component or servos with a one-way pump and a solenoid valve, which realises lightweight and improves the sustainable motion time. Once charged, the internal air can be recycled with the cooperation of the one-way pump and the solenoid valve, and the external air source is not required. Combined with trajectory planning, multi-degree-of-freedom limb motion experiments demonstrate the rationality of SASA and limb structure design.

Acknowledgement

This work is supported by the National Natural Science Foundation of China (Grant No. 51675124). The authors are very grateful to the reviewers for their valuable comments, which improved the paper.

References

[1] J. Pandey, N.S. Reddy, R. Ray, and S.N. Shome, Biological swimming mechanism analysis and design of robotic frog, *Proc. 2013 IEEE International Conf. on Mechatronics and Automation*, Takamatsu, Japan, 2013, 1726–1731.

[2] H. Chum, S. Felt, J. Garner, and *S.* Green, Biology, behavior, and environmental enrichment for the captive African clawed frog (Xenopus spp), *Applied Animal Behaviour Science, 143*(2–4), 2013, 150–156.

[3] W. Zhang, J.Z. Fan, Y.H.Y.L. ZhuQiu, and J. Zhao, A method for mechanism analysis of frog swimming based on motion observation experiments, *Advances in Mechanical Engineering*, (8), 2014, 1–13.

[4] J.Z. Fan, W. Zhang, B.W. Yuan, and G. Liu, Propulsive efficiency of frog swimming with different feet and swimming patterns, *Biology Open, 6*(4), 2017, 503–510.

[5] J.Z. Fan, B.W. Yuan, and Q.L. Du, Joint design and position servo control of frog inspired robot based on pneumatic muscle and reset spring, *Proc. IEEE International Conf. on Mechatronics and Automation (ICMA)*, Changchun, China, 2018, 1914–1919.

[6] J.Z. Fan, W. Zhang, P.C. Kong, H.G. Cai, and G.F. Liu, Design and dynamic model of a frog-inspired swimming robot powered by pneumatic muscles, *Chinese Journal of Mechanical Engineering*, *30*, 2017, 1123–1132.

[7] T. Ren, Y. Zhang, and Y.J. Li, Development of an active helical drive self-balancing in-pipe robot based on compound planetary gearing, *International Journal of Robotics and Automation,* (34), 2019.

[8] C. Laschi, B. Mazzolai, and M. Cianchetti, Soft robotics: Technologies and systems pushing the boundaries of robot abilities, *Science Robotics, 1*(1), 2016, 3690.

[9] Z. Cui and H.Z. Jiang, Design and implementation of thuniform robotic fish with variable body stiffness, *International Journal of Robotics and Automation*, 2017.

[10] C. Ma, F. Yu, and Z. Luo, Simulations and experimental research on a novel soft-terrain hexapod robot, *International Journal of Robotics and Automation, 30*(3), 2015, 247–255.

[11] Y.G. Zhu and B. Jin, Compliance control of a legged robot based on improved adaptive control: Method and experiments, *International Journal of Robotics and Automation, 31*(5), 2016, 366–373.

[12] X. Huang, K. Kumar, M.K. Jawed, A.M. Nasab, Z. Ye, W. Shan, and C. Majidi, Highly dynamic shape memory alloy actuator for fast moving soft robots, *Advanced Materials Technologies*, *4*(4), 2019, 1800540.

[13] Y. Tang, Q. Lei, X. Li, C.M. Chew, and J. Zhu, A frog-inspired swimming robot based on dielectric elastomer actuators, *Proc. IEEE/RSJ International Conf. on Intelligent Robots and Systems (IROS)*, Vancouver, BC, Canada, 2017, 2403–2408.

[14] Z. Yoder, N. Kellaris, C. Chase-Markopoulou, D. Ricken, S.K. Mitchell, M.B. Emmett, R.F.ff. Weir, J. Segil, and C. Keplinger, Design of a high-speed prosthetic finger driven by peano-HASEL actuators, *Frontiers in Robotics and AI*, *7*, 2020.

[15] H. Sun, N.Y. Wang, H. Jiang, and X.P. Chen, Flexible honeycomb pneunets robot, *International Journal of Robotics and Automation*, 2016.

[16] H. Zheng, M.L. Wu, and X.R. Shen, A pneumatic variable series elastic actuator-powered transtibial prosthesis, *International Journal of Robotics and Automation*, (6), 2020, 408–418.

[17] L. Manamanchaiyaporn, T.T. Xu, X.Y. Wu, and H.H. Qian, Roles of magnetic strength in magneto-elastomer towards swimming mechanism and performance of miniature robots, *International Journal of Robotics and Automation*, 2020, 162–170.

[18] K. Liu, Y. Wu, J.Q. Xu, Y. Wang, Z. Ge, and Y. Lu, Fuzzy sliding mode control of 3-DOF shoulder joint driven by pneumatic muscle actuators, *International Journal of Robotics and Automation, 34*(1), 2019, 38–45.

[19] M. Li, A. Pal, A. Aghakhani, A. Pena-Francesch, and *M.* Sitti, Soft actuators for real-world applications, *Nature Reviews Materials, 7*, 2022, 235–249.

[20] J.H. Zhang, H.X. Guo, T. Wang, and J. Hong, The design and motion analysis of a pneumatic omnidirectional soft robot, *International Journal of Robotics and Automatio*n, *32*(6), 2017, 569–576.

[21] J.M. Ramos-Arreguin, S. Tovar-Arriaga, J.E. Vargas-Soto, and M.A. Aceves-Fernandez, FPGA embedded PD control of a 1 Dof manipulator with a pneumatic actuator, *International Journal of Robotics and Automation*, 2016.

[22] A. Chen, R. Yin, L. Cao, C. Yuan, H. Ding, and W. Zhang, Soft robotics: Definition and research issues, *Proc. 24th International Conf. on Mechatronics and Machine Vision in Practice (M2VIP),* Auckland, New Zealand, 2017, 366–370.

[23] J.Z. Fan, S.Q. Wang, and Q.G. Yu, Experimental study on frog-inspired swimming robot based on articulated pneumatic soft actuator, *Journal of Bionic Engineering, 17*(2), 2020, 270–280.

[24] Y. Yang, Y. Chen, Y. Li, M.Z. *Chen,* and *Y.* Wei, bioinspired robotic fingers based on pneumatic actuator and 3D printing of smart material, *Soft Robotics, 4*(2), 2017, 147.

[25] Y. Wei, Y. Chen, T. Ren, Q. Chen, and C. Yan, A novel, variable stiffness robotic gripper based on integrated soft actuating and particle jamming, *Soft Robotics*, 2016.

[26] T. Kitamori, A. Wada, H. Nabae, and K. Suzumori, Untethered three-arm pneumatic robot using hose-free pneumatic actuator, *Proc. IEEE/RSJ International Conf. on Intelligent Robots & Systems*, Daejeon, Korea (South), 2016, 543–548.

[27] J.Z. Fan, S.Q. Wang, Q.G. Yu, and Y. Zhu, Swimming performance of the frog-inspired soft robot, *Soft Robotics.* 7(5), 2020, 615–626.

[28] P. Polygerinos, W. Zheng, J. Overvelde, K.C. Galloway, R.J. Wood, K. Bertoldi, and C.J. Walsh, Modeling of soft fiber-reinforced bending actuators, *IEEE Transactions on Robotics, 31*(3), 2015, 778–789.

[29] M. Wehner, R.L. Truby, D.J. Fitzgerald, B. Mosadegh, G.M. Whitesides, J.A. Lewis, and R.J. Wood, An integrated design and fabrication strategy for entirely soft, autonomous robots, *Nature, 536*(7617), 2016, 451–455.

[30] Y. Li, T. Ren, Y. Li, *Y.* Chen, *and* S.H. Choi, Untethered-bioinspired quadrupedal robot based on double-chamber precharged pneumatic soft actuators with highly flexible trunk, *Soft Robotics*, *8*(1), 2020, 97–108.

[31] Y. Chen and S. Choi, Precharged pneumatic soft actuators and their applications to untethered soft robots, *Soft Robotics*, 2018, 567–575.

[32] T. Ren, Y. Li, M. Xu, *Y. Li*, C. Xiong *and Y.*A. Chen, Novel tendon-driven soft actuator with self-pumping property, *Soft Robotics,* 7(2), 2019, 130–139.

[33] A. Tony, A. Rasouli, A. Farahinia, G. Wells, H. Zhang, S. Achenbach, S.M. Yang, W. Sun, and W. Zhang, Toward a soft microfluidic system: concept and preliminary developments, *Proc. 27th International Conf. on Mechatronics and Machine Vision in Practice (M2VIP),* Shanghai, 2021, 755–759.

Biographies

Shuqi Wang received the M.S. degree in mechanical manufacturing and automation from the Harbin University of Science and Technology, Harbin, China, in 2019. He is currently pursuing the Ph.D. degree with the School of Mechatronics Engineering, Harbin Institute of Technology, Harbin, China. His research interest includes soft robot and bionic robot.

Jizhuang Fan received the Ph.D. degree in mechanical engineering from the Harbin Institute of Technology (HIT), Harbin, in 2007. He is currently a Professor and a Ph.D. Supervisor with the School of Mechatronics Engineering, HIT. His main research interests include bionic robots and mechatronic devices.

Yitao Pan received the M.S. degree in mechanical engineering from Shandong University in 2020. He is currently pursuing the Ph.D. degree with the School of Mechatronics Engineering, Harbin Institute of Technology, Harbin, China. His current research interests include bionic robots and amphibious robot.

Yubin Liu received the Ph.D. degree in mechanical engineering from the Harbin Institute of Technology (HIT), Harbin, in 2007. He is currently a Professor and a Ph.D. Supervisor with the School of Mechatronics Engineering, HIT. His main research interests include bionic robots and cooperative robots.